ORIGINAL RESEARCH ARTICLES

IN SILICO STUDIES OF SOME NEWLY DESIGNED BENZIMIDAZOLE-THIAZOLIDINONE BASED ANTAGONISTS OF HUMAN ESTROGEN RECEPTOR

Jyoti Monga[a,b], Niladry S. Ghosh[a,c]*, Somdutt Mujwar[d] and Isha Rani[e]

(Received 26 May 2023) (Accepted 05 August 2023)

ABSTRACT

Breast cancer is globally associated with majority of the women. Indeed, high estrogen levels are the most common subtype of breast cancer. Three different classes of estrogen receptor antagonists are frequently used to treat such kinds of breast cancers. Each of these interacts directly with the initiation and activation of the estrogen signalling pathway. However, new medicines must be developed because resistance limits the therapeutic effectiveness. *In silico* studies for drug discovery have become popular in recent years due to their low cost and quick execution. To develop novel therapeutics for breast cancer, three different series of benzimidazole compounds targeting the estrogen receptor were docked. Among these three series, benzimidazole fused with pyrazole showed significant results and the leading compound was 32 based on docking results. The docking data was further validated by executing molecular dynamics (MD) simulations for the stability of designed leads within the macromolecular cavity in relation to time. Therefore, it is proposed that the pyrazole fused benzimidazole nucleus can be a promising pharmacophore for developing novel anticancer therapeutics for breast cancer.

Keywords: Molecular docking simulation, breast-cancer, thiazolidinone, estrogen receptor alpha, ADME, benzimidazole

INTRODUCTION

Non-communicable diseases (NCDs) accounted for more than 71% of deaths globally. In India, NCDs accounted for more than 63% of all deaths. Cancer is one of the leading causes of death from NCDs [1-2] .In 2020, more than 1.3 million cancer patients were reported in India[3]. The most prominent sites for carcinogenic growth are the breast, mouth, lungs, cervix, uterus and tongue. According to the WHO, 2.3 million new cases of breast cancer will be detected in 2020, resulting in 68,500 deaths from the disease. According to the report released by the Shri Shankara Cancer Foundation, out of the total of 29 different types of cancer, the most cases were of breast cancer reported during 2019–2021(Table I).

Table I: Cases of cancer reported in India during 2019-2021 as reported by Shri Shankara Cancer Foundation

Types of cancer	Year 2019	Year 2020	Year 2021
Breast cancer	1510	1167	1133
Lung cancer	353	329	283
Ovarian cancer	211	340	134
Lymphoma cancer	257	212	172
Prostate cancer	272	166	172

The steroid hormone, estradiol, is involved in the progression of breast cancer[4]. Differentiation and maintenance of reproductive tissues, muscles and other tissues is regulated by the binding of estrogen to their receptors (ERs). Binding of ligands to ER alpha regulates target gene expression. ER agonist binding in breast

[a] Department of Pharmaceutical Chemistry, Adarsh Vijendra Institute of Pharmaceutical Sciences, Shobhit University, Gangoh – 247 341, Uttar Pradesh, India

[b] Department of Pharmaceutical Chemistry, Ch. Devi Lal College of Pharmacy, Jagadhri-135 003, Haryana, India

[c] Department of Pharmaceutical Chemistry, Faculty of Pharmaceutical Sciences, Assam Downtown University, Guwahati-781 026, Assam, India

[d] Department of Pharmaceutical Chemistry, Chitkara College of Pharmacy, Chitkara University, Rajpura-140 401 Punjab, India

[e] Department of Pharmaceutical Chemistry, Spurthy College of Pharmacy, Marasur Gate, Bengaluru, Raj – 562 106, Karnataka, India

*For Correspondence: E-mail: ghoshniladry@gmail.com

https://doi.org/10.53879/id.60.08.14087

cancer cells can create a transcriptional co regulator, because when it is antagonistic, the ER will actively create the corepressors, thereby causing transcriptional suppression of the target genes[5-6]. There are generally two methods to inhibit the progression of breast cancer: an aromatase inhibitor, which inhibits estrogen production[7], and selective estrogen receptor modulators (SERMs), which specifically impede the signalling of genomic estrogen. Aromatase inhibitors can only work against postmenopausal breast cancer[8].

There are numerous medicines on the market, such as anastrozole. Setti *et al.* revealed the Mol Dock score of anastrozole to be -19.521 kcal mol^{-1} [9]. Tilak Vijay *et al.* and Verma *et al.* reported the Mol Dock scores of tamoxifen (Fig. 1) and letrozole (Femara) to be -149.856 and –136.784 kcal mol^{-1}, respectively. Nolvadex and Soltamox[10] are two commonly used brand names for the medication tamoxifen. However, they come with shortcomings like the development of endometric carcinoma, thrombosis in the legs and lungs, strokes, and myopia. Letrozole is an aromatase inhibitor (AIs) but it causes polycystic ovary syndrome (PCOS)[11].

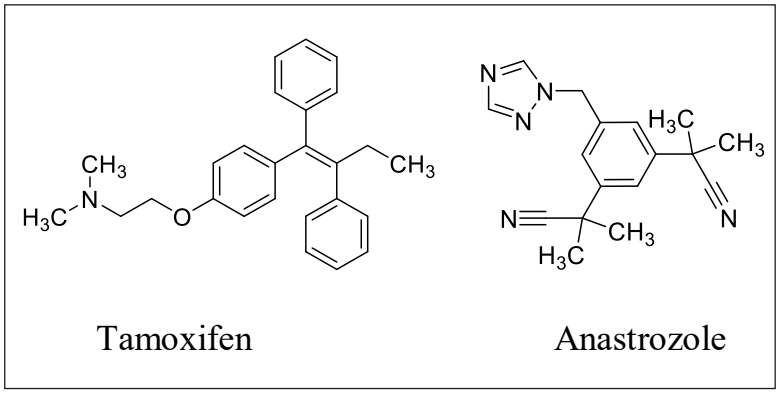

Fig. 1: Chemical structures of marketed drugs used to treat cancer

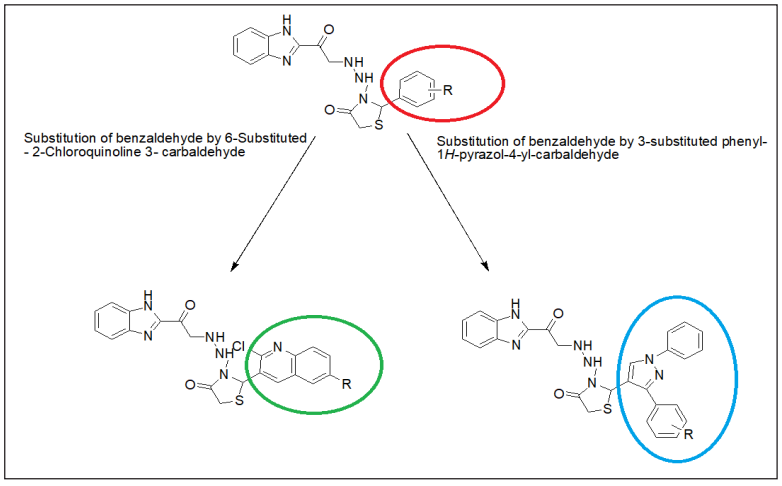

Fig. 2: Structural modification in 2-substituted benzimidazole

This research was aimed to find new benzimidazole compounds with anti-estrogen receptor alpha activity for application in the treatment of breast cancer. In the present article, we describe various benzimidazole derivatives and their potential to link with ERα-positive sites, which were obtained from the Protein Data Bank. In addition, we used molecular dynamics to investigate the stability of the complex across time, as well as docking score comparisons with already available medications used to treat breast cancer and ADME analyses here on ligands.

2-SUBSTITUTED BENZIMIDAZOLE AS ANTI-CANCER AGENTS

Through a variety of modes of action, including DNA alkylation, DNA binding, interfering with tubulin polymerization or depolymerization, enzyme inhibition, antiangiogenic effects, and signal transmission, benzimidazole has demonstrated its anticancer activity. The protein target used in this docking research was PDB ID: 3ERT, which was accessed from http://www.rscb.org/pdb[12].

METHODOLOGY

Computational approaches have been extremely useful in coming up with workable solutions to the diverse sampling issue. Sinces it is impossible to create and analyse every potential chemical, molecular modelling simplifies this method and restricts the number of compounds to a set number[13,14]. The following stages are involved:

- Choosing a data set
- Prepare the ligands
- Protein preparation
- Docking
- Binding energy calculations

Data set selection

With the design of fictitious benzimidazole compounds (Fig. 2) docking investigations were conducted. The basic structure of analogues is shown below (Table II-IV).

Protein and ligand preparation

The protein estrogen receptor alpha was downloaded from Protein Data Bank[12] (http://

Table II: 2-substituted benzimidazole thiazolidinone derivatives containing quinoline as moiety

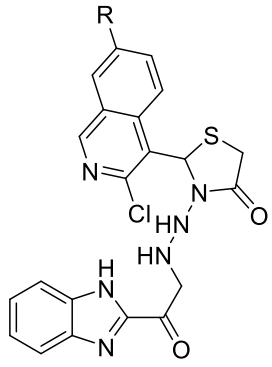

Compound No.	R-group
1	H
2	CH_3
3	Cl
4	Br
5	F
6	OH
7	OCH_3
8	NH_2
9	NO_2
10	$OCOCH_3$
11	SO_3H

Table III: 2-substituted benzimidazole thiazolidinone derivatives containing pyrazole as substituent

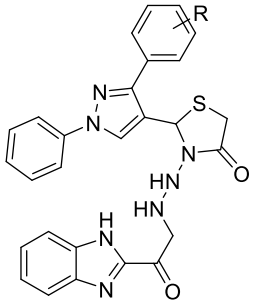

Compound No.	R-group
12	H
13	4-CH_3
14	4- Cl
15	4-Br
16	4-F
17	4-OH
18	4-OCH_3
19	4-NH_2
20	4-NO_2
21	4-$OCOCH_3$
22	4-SO_3H
23	4-OCF_3
24	3-CH_3
25	3-SO_3H
26	3-Cl
27	3-F
28	3-Br
29	3-OH
30	3-OCH_3
31	3-NH_2
32	3-$OCOCH_3$

Table IV: 2-substituted benzimidazole thiazolidinone derivatives containing substituted benzaldehyde as substituent moiety

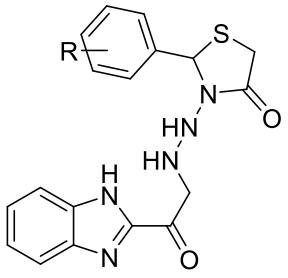

Compound No.	R-group
33	H
34	4-Cl
35	4-OH
36	4-NO_2
37	4-NH_2
38	4-F
39	4-OCH_3
40	4-CH_3
41	4-isopropyl

42	4-tert. butyl
43	3-Cl
44	3-OH
45	3-NO_2
46	3-NH_2
47	3-F
48	3-$OCOCH_3$
49	3-OCH_3
50	3-CH_3
51	2-Cl
52	2-OH
53	2-NH_2
54	2-F
55	2-$OCOCH_3$
56	2-OCH_3
57	2-CH_3

www.rscb.org/pdb). Furthermore, some of the amino acids in the retrieved protein have been interrupted, and these have been repaired and recreated using mutation and optimization approaches[15]. ACD Chem Sketch 12 was used to prepare the ligands and convert them from 2D to 3D structures utilizing construction and optimization techniques, and then the advanced structures were cleaned. The MDL Molfile (mol) format was used to store

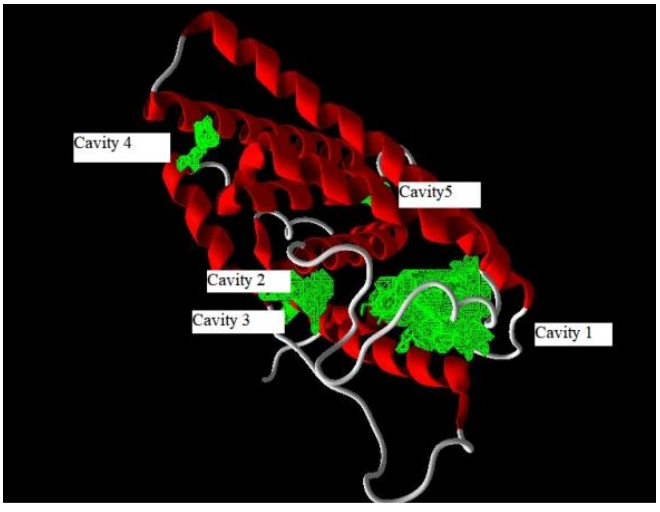

Fig. 3: MVD detect five binding sites in the protein structure of estrogen receptor alpha

the resultant structures. The constructed 3D structures were then imported into the Molegro Virtual Docker 6.0 v. The imported structures must be adequately prepared to provide accurate predictions, which involves ensuring the correct atom connectivity and bond ordering. Cofactors and water molecules found in proteins downloaded from the protein data bank must be deleted from the MVD workspace before docking in order to avoid inaccurate results. The receptor location is then covered with an electrostatic surface.

Cavity or active site prediction

The docking process comprises a vital activity called cavity identification. A grid-based cavity prediction system was created to identify the likely binding sites. Additionally, since the volume was chosen between 5 and 10,000, the cube with the maximum number of cavities was 30 × 30 × 30 $Å^3$, the cavity with the highest value among the five selected cavities was chosen for further consideration throughout the docking procedure primarily for ERα +Cavity 1 with volume (363.52$Å^3$) and surface area (819.2$Å^2$), respectively. All discovered cavities and the corresponding volume and surface area data are described in Table V and Fig. 3.

Table V: Binding cavities (1–5) inside Erα+(PDB ID: 3ERT) and their few parameters

PDB ID	Cavity no.	Surface area ($Å^2$)	Volume ($Å^3$)
3ERT	1	819.2	363.52
	2	166.4	55.808
	3	144.64	36.352
	4	64	15.36
	5	55.04	13.312

Molecular docking

Docking is a computational method for predicting the modes of action of organic molecules on protein receptors. It builds a grid of interaction points that represent the active spot in an image. It fits the ligand in the binding site of the receptor. The binding energy is calculated by taking into account several receptor-ligand interactions, such as Van der Waal's interaction, electrostatic interactions, and aromatic interactions[16,17]. All of the ligands optimised conformers were added to the docking wizard's workspace to begin docking. All the ligands were chosen in the docking wizard, and the grid resolution for the scoring function was changed to 0.30[18,19]. Then these three coordinates X (93.22), Y (59.12), and Z (52.34) were used to define the binding site, while its radius was adjusted to a value of 15.

The search algorithms were previously running ten times. By using a particular algorithm and a 12-6 conceivable and Lennard Jones' term "sp^2-sp^2 torsion," this operation was carried out by the software[20-24]. The docking script was finally created and launched into the workspace as an external process. The output directory contained the created script, log file, and constructed postures. In order to achieve ligand docking, a ligand is generated in a variety of orientations (or poses) within the active site. These poses are scored in order to select one or more poses that closely resemble the bioactive conformation identified by X-ray crystallography. Additionally, plausible binders from virtual chemical databases are identified using docking techniques, and the binding affinities of protein-ligand complexes are estimated. The ligand's optimal conformation or pose, which had the lowest Mol Dock score, was chosen to analyse binding interactions such as hydrogen bonds and steric interactions[19].

Calculation of the binding energy

$$Escore = Einter + Eintra \quad \text{---------1}$$

$$Einter = \sum i=ligand \sum j=protein [EPLP (rij) + 332.0\ qiqj\ \ 4r^2ij \quad \text{---------2}$$

$$Eintra = \sum i=ligand \sum j=protein [EPLP (rij)] + \sum \text{flexible bond A } [1 - \cos (m\theta - \theta \circ)] + Eclash \quad \text{----3}$$

The differential algorithm can be used to calculate the MolDock score. Equation 1 represents the total binding affinity (Escore), and the term Einter refers to the ligand and receptor energy interaction, and Eintra shows the ligand internal energy. Eqs. 2 and 3 are also used to compute the Einter and Eintra. However, the steric interaction of charged atoms was studied using the piecewise linear potential (EPLP)[25]. The energy of the pair of atoms in the ligand is described by the first term in Eq. 3, although this only applies to single bonds. The second term of the equation, which stands for the bond's torsional angle, has been used to represent the torsional energy. If the number of torsions could be determined, the torsional energy average could be calculated. When two dense atoms are closer together than 2.0, the third term, "Eclash," is used and a penalty of 1000 kcal mol^{-1} is applied.

Molecular dynamics simulation

The Desmond module of the Schrodinger programme was used to simulate the human estrogen receptor macromolecular complex for 100 ns with compound 32 to assess the binding patterns and stability of the leads selected by simulated screening. An orthorhombic-shaped simulation box with a 10-gap between the box wall and the ligand-protein combination was made using the TIP3P explicit water model. The isosmotic environment in the simulation box was made by introducing counter ions and neutralising the charge using 0.15 M NaCl[26-29]. The system's energy was decreased by doing 2000 repeats using a 1 kcal mol^{-1} merging threshold. An energy-minimized complex system was used to run a 100 ns MD simulation. A constant pressure of 1.013 bars and temperature of 300 K were used throughout the simulation procedure. The trajectory route has been set at 9.6 with an energy interval of 1.2 ps, so that simulation interaction graphs may be built after the simulation procedure.

ADME/ PHARMACOKINETIC STUDIES

Docking studies do not reveal the suitability of a drug to be potent. Swiss ADME software has conducted druglikeness analysis and ADME (absorption, distribution, metabolism, and excretion) analysis, which helps to determine whether medication may be utilised for biological reasons. The Swiss Institute of Bioinformatics (SIB) has launched the new and expensive webtool SwissADME to promote bioinformatics resources and services for scientists all over the world[30,31]. The ligands are loaded into the programme using SMILES (Simplified Molecular Input Line Entry System) to construct the pharmacokinetic profile[32].Swiss ADME was used to generate the ADME profile for compounds 12 to 32. Additionally, the Lipinsky rule of five was created in 1997 as a precise benchmark to identify pharmacological similarities. A drug may be absorbed into the body through oral absorption if two or more of the following criteria are satisfied: the molecule's molecular weight (MW) must be less than 500 g moL^{-1}; the iLogP (octanol/water partition coefficient) must be 5; the nHBD (H-bond donor) and nHBA (H-bond acceptor) must be in the range of 10 and 5, respectively[33]. The following is how the Ghose filter defines druglikeness restriction: The computed MW varies from 354 to 433, the molar refractivity ranges from 117 to 127, and the total number of atoms ranges from 27 to 30. The calculated log P value ranges from 3.92 to 5.57. While, according to the Veber rule, drug-likeness constraints are rotatable bond count i.e 10 and polar surface area (PSA) 140. Insoluble (-10), weakly soluble (-6), moderately soluble (-4), soluble (-2) or very soluble (0) are the several categories of solubility in water. The medicinal property was also tested by Molinspiration software.

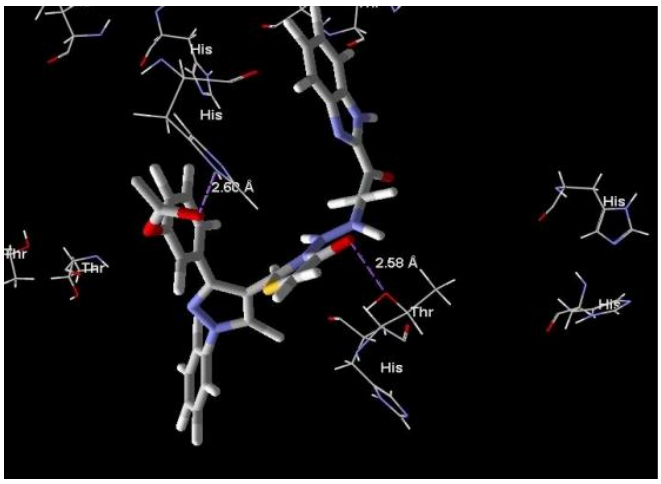

Fig. 4: Compound 32 docked into ERalpha, MolDock score -178.021, Dotted Purple line represent hydrogen bond interaction between compound and protein residues

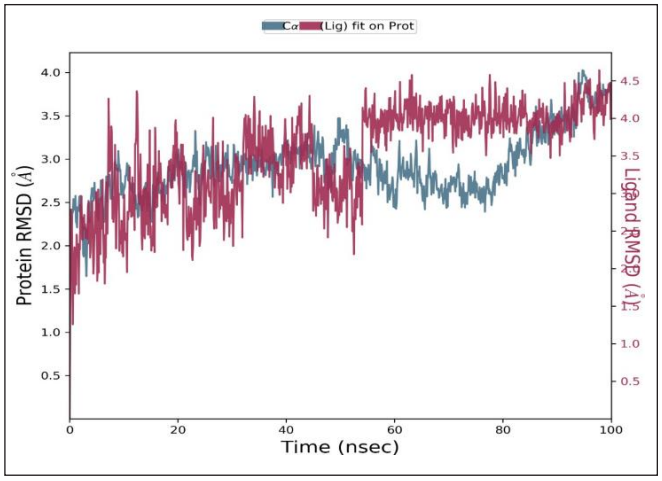

Fig. 5: Root mean square error of estrogen complexes as a function of time

Table VI: Docking scores of benzimidazole thiazolidinone derivatives having quinoline as substituent using PDB ID: 3ERT for anticancer activity

Sr. No.	R-group involved	Mol dock score	Docking score	H-bonds	H-bond distance (Å)	Interacting protein residue	Interacting ligand molecule
Standard	**OHT_600[A]**	**-149.766**	**-90.31**	**3**	**3.51**	**O of Phe 404**	**O of OH**
					2.55	**N of Arg 394**	**O of OH**
					2.89	**O of Glu 353**	**O of OH**
1	H	-134.512	-88.66	1	2.99	O of Thr 347	O of C=O
2	CH_3	-132.457	-86.62	1	2.91	O of Thr 347	O of C=O
3	Cl	-123.29	-84.24	2	3.10	O of Thr 347	O of C=O
					3.24	O of Leu 346	N of NH
4	Br	-128.94	-85.49	1	2.80	O of Thr 347	O of C=O
5	F	-120.82	-81.48	0	-	-	-
6	OH	-133.843	-88.81	2	2.83	O of Thr 347	O of C=O
					2.31	N of Arg 394	O of OH
7	OCH_3	-123.118	-77.12	1	2.60	O of Thr 347	=O of thiazolidinone
8	NH_2	-137.515	-90.49	2	2.94	O of Thr 347	O of C=O
					2.30	N of Arg 394	N of NH_2
9	NO_2	-124.59	-77.69	3	2.79	O of Leu 346	N of NH of imidazole =O of thiazolidinone -O of NO_2
					2.61	O of Thr 347	
					3.03	N of Trp 383	
10	$OCOCH_3$	-111.32	-76.14	1	2.70	O of Thr 347	=O of thiazolidinone
11	SO_3H	-120.91	-93.455	3	2.97	O of Leu 346	N of NH of imidazole =O of SO_3H =O of thiazolidinone
					3.05	N of Trp 383	
					2.56	O of Thr 347	

Table VII: Docking scores of benzimidazole thiazolidinone derivatives having pyrazole as substituent using PDB ID: 3ERT for anticancer activity

Sr. No.	R-group involved	Mol dock score	Docking score	H-bonds	H-bond distance (Å)	Interacting residue	Interacting ligand
Standard	**OHT_600[A]**	**-149.766**	**90.31**	**3**	**3.51** **2.55** **2.89**	**O of Phe 404** **N of Arg 394** **O of Glu 353**	**O of OH** **O of OH** **O of OH**
12	H	-147.88	-79.60	1	3.02	O of Asp 351	N of NH of imidazole
13	CH_3	-142.026	-74.68	0	-	-	-
14	Cl	-158.65	-62.67	1	2.61	O of Leu 346	N of NH of imidazole
15	Br	-138.193	-83.79	2	2.68 2.60	O of Leu 346 O of Thr 347	N of NH of pyrazole =O of thiazolidinone
16	F	-153.441	-89.87	1	2.91	O of Thr 347	=O of thiazolidinone
17	OH	-149.959	-82.69	1	2.79	O of Thr 347	=O of thiazolidinone
18	4-OCH_3	-122.366	-50.06	2	3.43	N of His 524	O of OCH_3
19	4-NH_2	-155.53	-71.25	2	3.17 3.50	N of His 524 O of Asp 351	N of NH_2 N of NH of imidazole
20	4-NO_2	-149.53	-49.26	3	3.21 2.60	=O of thiazolidinone -O of NO_2	O of Thr 347 N of Leu 536
21	4-$OCOCH_3$	-136.837	-33.58	4	3.13 2.94 2.59 2.92	O of Glu 353 O of Leu 387 N of Arg 394 O of Glu 353	N of NH of imidazole N of NH =O of C=O N of NH
22	4-SO_3H	-114.484	-63.38	1	2.81	O of Thr 347	=O of thiazolidinone
23	4-OCF_3	-161.173	-55.52	0	-	-	-
24	3-CH_3	-148.84	-82.11	1	3.13	O of Thr 347	=O of thiazolidinone
25	3-SO_3H	-156.36	-83.11	1	2.66	O of Thr 347	=O of thiazolidinone
26	3-Cl	-167.51	-71.34	2	2.48 2.63	O of Glu 353 O of Glu 353 N of Leu 391	N of NH of imidazole N of NH O of C=O
27	3-F	-130.62	-76.07	1	2.71	O of Thr 347	=O of thiazolidinone
28	3-Br	-162.10	-73.85	0	-	-	-
29	3-OH	-158.43	-91.35	1	3.06	O of Thr 347	=O of thiazolidinone
30	3-OCH_3	-155.529	-47.19	2	2.79 3.04	O of Thr 347 O of Thr 347	=O of thiazolidinone =O of C=O
31	3-NH_2	-161.51	-80.38	0	-	-	-
32	3-$OCOCH_3$	-178.021	-63.00	2	2.58 2.60	O of Thr 347 N of His 524	=O of thiazolidinone =O of $OCOCH_3$

Table VIII: Docking scores of benzimidazole thiazolidinone derivatives having benzaldehyde as substituent using PDB ID: 3ERT for anticancer activity

Sr. No.	R-group involved	Mol dock score	Docking score	H-bonds	H-bond distance (Å)	Interacting residue	Interacting molecule
Standard	**OHT_600[A]**	**-149.766**	**90.31**	**3**	**3.51** **2.55** **2.89**	**O of Phe 404** **N of Arg 394** **O of Glu 353**	**O of OH** **O of OH** **O of OH**
33	H	-77.72	-105.27	0	-	-	-
34	4-Cl	-86.32	-108.24	1	2.92	O of Leu 346	-N of NH
35	4-OH	-78.86	-118.37	0	-	-	-
36	4-NO_2	-76.74	-125.24	3	3.38 2.63 3.01	N of Arg 394 N of Arg 394 =O of C=O	- N of NO_2 =O of NO_2 =O of C=O
37	4-NH_2	-83.48	-131.42	2	2.58 3.07	N of Arg 394 O of Thr 347	-N of NH_2 =O of C=O
38	4-F	-85.54	-127.766	1	3.15	O of Thr 347	=O of C=O
39	4-OCH_3	-79.477	-127.297	2	2.80 3.22	N of Arg 394 O of Thr 347	-O of OCH_3 -N of NH
40	4-CH_3	-85.45	-126.23	1	3.50	O of Thr 347	=O of C=O
41	4-isopropyl	-80.08	-132.75	1	2.66	O of Thr 347	=O of C=O
42	4-tert butyl	-73.70	-122.85	0	-	-	-
43	3-Cl	-84.74	-136.05	2	2.60 2.94	O of Thr 347 O of Leu 346	=O of thiazolidinone N of NH of imidazole
44	3-OH	-79.22	-133.63	2	2.93 2.90	O of Thr 347 N of Arg 394	=O of C=O -O of OH
45	3-NO_2	-73.25	-141.906	2	2.77 3.05	O of Thr 347 N of Arg 394	=O of C=O -O of NO_2
46	3-NH_2	-76.93	-129.89	2	3.10 2.60	O of Leu 346 O of Thr 347	-N of NH of imidazole =O of thiazolidinone
47	3-F	-83.51	-132.37	1	2.60	O of Thr 347	=O of C=O
48	3-$OCOCH_3$	-72.46	-133.218	2	2.83 2.73	O of Thr 347 O of Leu 346	=O of thiazolidinone
49	3-OCH_3	-74.14	-131.41	2	2.82 3.10	N of Arg 394 O of Thr 347	-O of OCH_3 =O of C=O

50	3-CH_3	-80.04	-129.158	0		-	-
51	2-Cl	-82.09		2	2.66 3.02	O of Thr 347 O of Leu 346	=O of thiazolidinone -N of NH of imidazole
52	2-OH	-82.91	-126.20	2	2.68 3.07	O of Thr 347 O of Leu 346	=O of thiazolidinone -N of NH of imidazole
53	2-NH_2	-78.93	-123.66	2	3.10 3.10	O of Thr 347 O of Thr 347	=O of C=O N of imidazole
54	2-F	-81.93	-126.091	1	2.81	O of Thr 347	=O of C=O
55	2-$OCOCH_3$	-71.91	-131.21	1	3.13	O of Thr 347	=O of C=O
56	2-OCH_3	-82.79	-127.59	1	2.64	O of Thr 347	=O of thiazolidinone
57	2-CH_3	-82.37	-133.82	1	2.69	O of Thr 347	=O of C=O

RESULTS AND DISCUSSION

Docking studies

A molecular docking research was conducted to examine the compounds' modes of binding to the human estrogen receptor alpha. Virtual scans of the estrogen receptor alpha binding site for 57 designed derivatives and standard 4-hydroxy tamoxifen for cancer were conducted, and the outcomes were contrasted with those of dockings with the approved anticancer drug 4-hydroxy tamoxifen using the same cavity site. The molecular docking data that were shown in terms of negative energy value suggested that lower the binding energy value, binding affinity with the receptor would be optimal. Tables VI, VII, and VIII show the MolDock score and H-bonding between breast cancer proteins and ligands (57 hypothetically designed benzimidazoles). Benzimidazole with pyrazole exhibited better binding affinity as compared to compounds with quinoline and substituted benzaldehyde as a substituent, and the most potent compounds in the pyrazole series was 32 with MolDock score of (-178.021); binding analysis is shown in Fig. 4.

Molecular dynamic simulation

Using MD modelling using the Schrodinger-Desmond programme, it was shown that the purported inhibitor (32) comprised of 41 heavy atoms out of a total of 100 atoms, had a macromolecular connection with the human nociception receptor made up of 246 amino acids and was stable over time. The stability and structural alterations of the protein backbone were estimated using the RMSD during the course of the simulation. Following the application of MD simulation to the macromolecular complex containing 32, (3-2-[2-(1*H*-benzimidazol-2-yl)-2-oxoethyl] hydrazino-2-(3-acetoxyphenyl-1-phenyl-1*H*-pyrazol-4-yl)-1,3-thiazolidin-4-one), the obtained

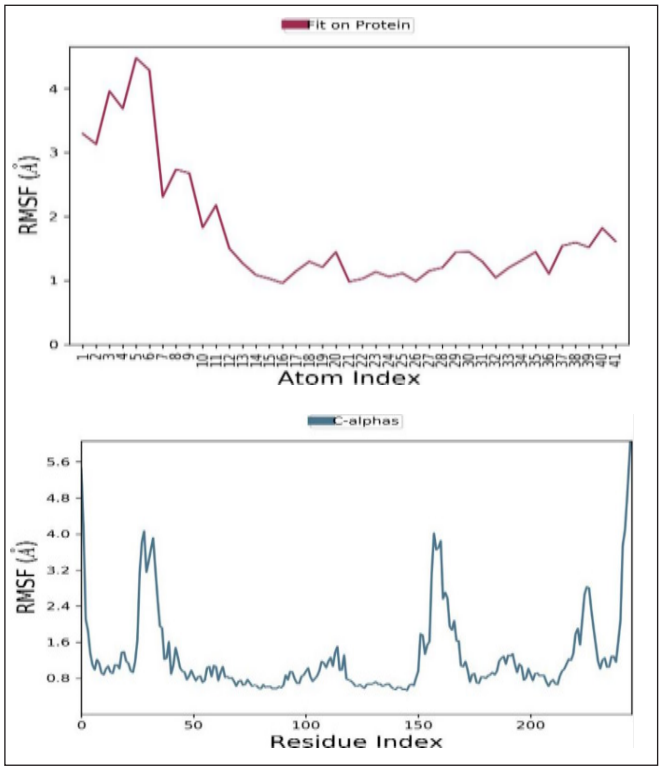

Fig. 6: Human estrogen receptor and complexed ligand compound 32, RMSF (Root mean square fluctuation)

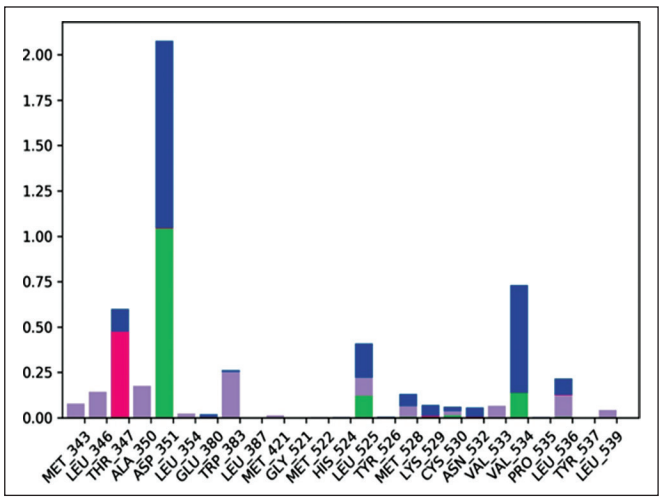

Fig. 7: Receptor-drug contacts: during an MD simulation with a timeframe of 100 ns, the human estrogen receptor made receptor-drug contacts with the ligand compound 32. Green bars stand for hydrogen bonds, blue bars for water bridges, and purple bars for hydrophobic interactions

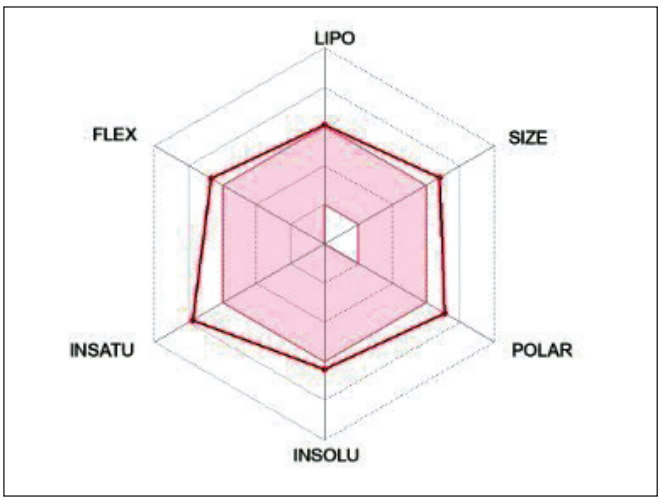

Fig. 8: Bioactivity radar of hypothetically designed pyrazole based benzimidazole (32)

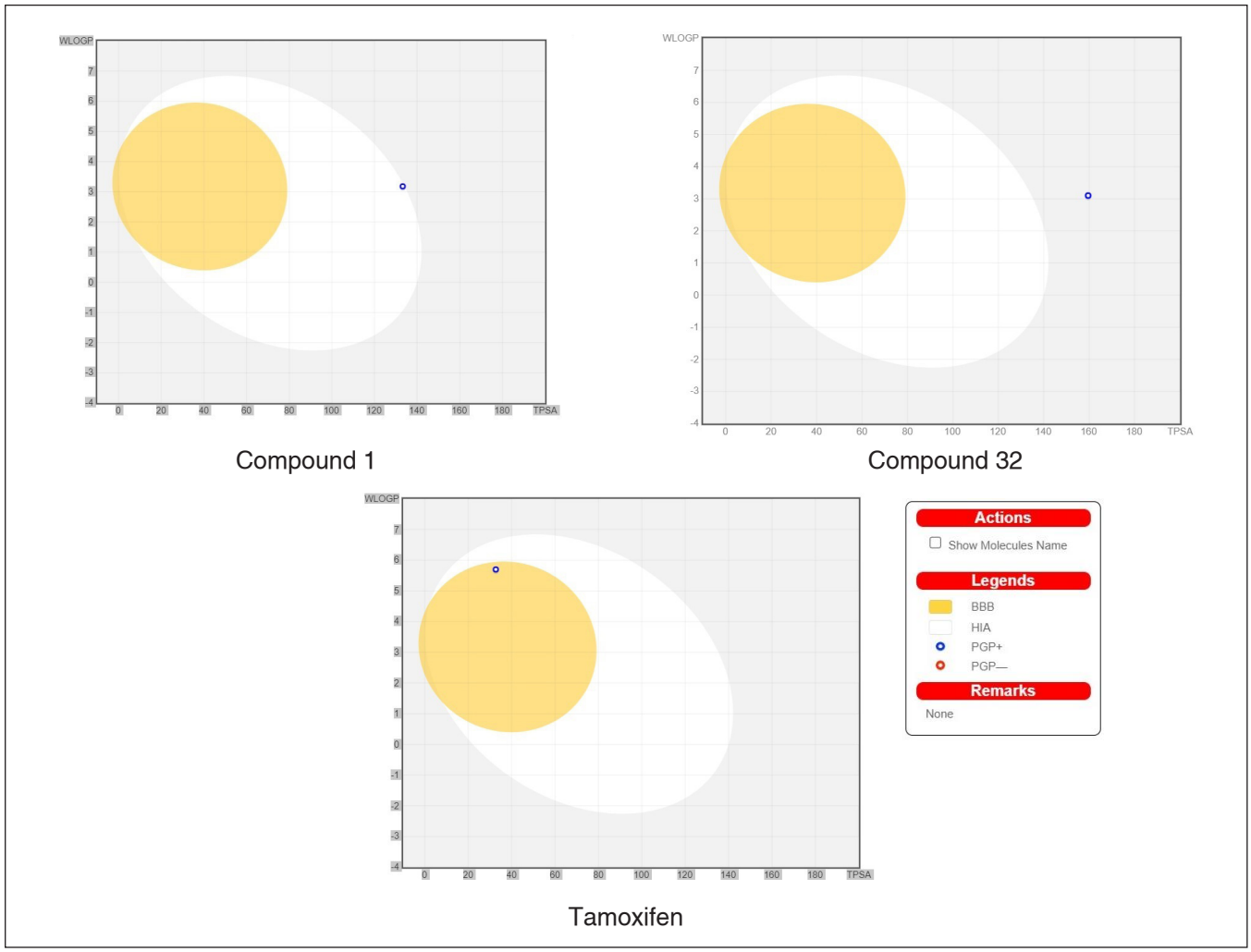

Fig. 9: Boiled-Egg diagram of compound 1, 32 and reference tamoxifen

Table IX: Physicochemical properties of hypothetically designed benzimidazole thiazolidinone derivatives having pyrazole as substituent (12-32)

Comp. No.	MW	%ABS	Log $P_{o/w}$	n-HBA	n-HBD	Mol. Ref	LogS (ESOL)	TPSA (Å)	n violation	No. of rotational bond
Tamoxifen	**371.51**	**67.7**	**5.77**	**2**	**0**	**119.72**	**-6.59**	**12.47**	**1**	**8**
12	509.58	63.1	3.23	6	3	145.85	-6.38	133.24	1	8
13	523.61	63.1	3.68	6	3	150.81	-6.68	133.24	1	8
14	544.03	63.1	3.88	6	3	150.86	-6.97	133.24	1	8
15	588.48	63.1	3.96	6	3	153.55	-7.29	133.24	1	8
16	527.57	63.1	3.66	7	3	145.8	-6.54	133.24	1	8
17	525.58	56.1	2.94	7	4	147.87	-6.24	153.47	1	8
18	539.61	59.9	3.31	7	3	152.34	-6.46	142.47	1	9
19	524.6	54.9	2.79	6	4	150.25	-6.03	159.26	1	8
20	554.58	47.3	2.55	8	3	154.67	-6.45	179.06	2	9
21	567.62	53.96	3.26	8	3	157.34	-6.4	159.54	2	10
22	589.65	41.4	1.93	9	4	155.7	-4.53	195.99	2	9
23	593.58	59.9	4.05	10	3	152.53	-7.45	142.47	1	10
24	523.61	63.1	3.57	6	3	150.81	-6.68	133.24	1	8
25	589.65	41.4	1.9	9	4	155.7	-4.53	195.99	2	9
26	544.03	63.1	3.92	6	3	150.86	-6.97	133.24	1	8
27	527.57	63.1	3.7	7	3	145.8	-6.54	133.24	1	8
28	588.48	63.1	3.95	6	3	153.55	-7.29	133.24	1	8
29	525.58	56.1	2.92	7	4	147.87	-6.24	153.47	1	8
30	539.61	59.9	3.35	7	3	152.34	-6.46	142.47	1	9
31	524.6	54.1	2.6	6	4	150.25	-6.03	159.26	1	8
32	567.62	53.96	3.36	8	3	157.34	-6.4	159.54	2	10

trajectories revealed that the complex was stable throughout the 100-ns simulation, with an average RMSD for the macromolecular backbone ranging from 1.5 to 4.0 Å. The RMSD value of the ligand has been maintained within the 3.0-4.5 range throughout the simulation run, with very few changes up to 4.5 for altering the ligand within the receptor's cavity. Compound 32 makes a few slight adjustments after it binds to the human estrogen receptor's active site in order to achieve continuous affirmation there. The constant behaviour of the complex ligand compound 32 and the macromolecular backbone is seen in Fig. 5 with very little volatility.

To assess the vibrations of the amino acids in reference to their initial conformation, the RMSF value of the target receptor was taken into consideration through monitoring the change of C atoms in the peptide chain. The RMSF value of the macromolecular backbone was found to range from 0.8 to 4.0. Analysis revealed that the complex system's RMSF value was lower for the active amino acids and that the ligand compound 32 mean alteration ranged from 1.0 to 4.0, indicating that the macromolecular active site has acceptable variations. RMSF of macromolecules' C backbones as well as the complex ligand compound 32 were seen during the 100 ns MD simulation period shown in Fig. 6.

Table X: Pharmacokinetics of hypothetically designed benzimidazole thiazolidinone derivatives having pyrazole as substituent (12-32)

Comp. No.	GI absorption	BBB Permeant	P-Gp	CYP 1A2	CYP2C 19	CYP2 C9	CYP2 D6	CYP3 A4	Log Kp (skin permeation) cm s^{-1}
Tamoxifen	**Low**	**No**	**Yes**	**No**	**Yes**	**No**	**Yes**	**No**	**-3.5**
12	High	No	Yes	No	Yes	Yes	Yes	Yes	-5.59
13	Low	No	Yes	No	Yes	Yes	Yes	Yes	-5.42
14	Low	No	No	No	Yes	Yes	Yes	Yes	-5.36
15	Low	No	No	Yes	Yes	Yes	Yes	Yes	-5.58
16	Low	No	Yes	No	Yes	Yes	Yes	Yes	-5.63
17	Low	No	No	No	Yes	Yes	No	Yes	-5.94
18	Low	No	Yes	No	Yes	Yes	Yes	Yes	-5.79
19	Low	No	Yes	No	Yes	Yes	No	Yes	-6.16
20	Low	No	Yes	No	Yes	Yes	No	Yes	-5.98
21	Low	No	Yes	No	Yes	Yes	No	Yes	-6.12
22	Low	No	No	No	No	No	No	No	-8.59
23	Low	No	No	No	Yes	Yes	No	Yes	-5.26
24	Low	No	Yes	No	Yes	Yes	Yes	Yes	-5.42
25	Low	No	No	No	No	No	No	No	-8.59
26	Low	No	No	No	Yes	Yes	Yes	Yes	-5.36
27	Low	No	Yes	Yes	Yes	Yes	Yes	Yes	-5.63
28	Low	No	No	Yes	Yes	Yes	Yes	Yes	-5.58
29	Low	No	No	No	Yes	Yes	No	Yes	-5.94
30	Low	No	Yes	No	Yes	Yes	Yes	Yes	-5.79
31	Low	No	No	No	Yes	Yes	No	Yes	-6.16
32	Low	No	Yes	No	Yes	Yes	No	Yes	-6.12

The macromolecular structure contained a total of 56.88% SSE, of which 53.47% were alpha helices and 3.20% were beta sheets, which were maintained during the simulation process, according to the SSE study. The stability of the protein ligand complex is provided through the creation of hydrogen bonds, hydrophobic contacts, and ionic interactions during the MD simulation. To gauge the stability of the ligand compound 32, the strength of these connections was tracked over the whole simulation timeframe. The simulation process looked at how compound 32, a ligand, and the human estrogen receptor interacted. It has been demonstrated that the amino acids Met343, Leu346, Ala350, Leu525, Val533, Leu536, and Leu539 make a hydrophobic interaction with hydroxy molecules, whereas Asp351, Leu525, and Val534 form a hydrogen bond with them. The interaction of the ligand compound 32 with the macromolecular target estrogen receptor is shown in Fig.7. During the simulated session, interactions between bound ligands and more than six residues were ongoing. For the assured ligand compound 32, the rGyr value fell between 4.8 and 5.6 2. The ligand's MolSA was determined to be between 525 and 555 $Å^2$. After some early changes, the ligand's SASA was found to be in the range of 160-400 $Å^2$, whereas the complex ligand's PSA remained within the range of 160-200 $Å^2$ throughout the simulation procedure.

ADME Properties

In the human body, physicochemical and pharmacokinetic factors control how drugs are distributed.

Table XI: Druglikeness of hypothetically designed benzimidazole thiazolidinone derivatives having pyrazole as substituent (12-32)

Comp. No.	Lipinski: No. of violations	Ghose: No. of violations	Veber: No. of violations	Egan: No. of violations	Muegge	Bioavailability score
4-hydroxy tamoxifen	**1**	**1**	**0**	**1**	**1**	**0.55**
12	1	2	0	1	1	0.55
13	1	2	0	1	1	0.55
14	1	2	0	1	1	0.55
15	1	2	0	1	1	0.55
16	1	2	0	1	1	0.55
17	1	2	1	1	2	0.55
18	1	2	1	1	1	0.55
19	1	2	1	1	1	0.55
20	2	2	1	1	2	0.17
21	2	2	1	1	2	0.17
22	2	2	1	1	1	0.17
23	1	2	1	1	1	0.55
24	1	2	0	1	1	0.55
25	2	2	1	1	1	0.17
26	1	2	0	1	1	0.55
27	1	2	0	1	1	0.55
28	1	2	0	1	1	0.55
29	1	2	1	1	2	0.55
30	1	2	1	1	1	0.55
31	1	2	1	1	1	0.55
32	2	2	1	1	2	0.55

These features were forecast using the Swiss ADME webtool[32]. The physicochemical, pharmacokinetic, and pharmacodynamic characteristics of the strong chemicals (12-32) as predicted by Swiss ADME are listed in Tables IX, X, XI, and XII. According to the ADME prediction results (Table IX), all compounds (12-32) violated 1-2 of the drug likeness rules. As stated in the results, all the compounds are having molecular wt. > 500 and are poorly soluble in water. The intestinal absorption rate for all ligands from 12 to 32 spans between 41.4 to 63.1%, which is within the acceptable range of human intestinal absorption (%), which should not be < 30%. Moreover, through the Swiss ADME web server, the bioavailability radar of the compound 32 is represented in Fig. 8 based on physicochemical properties[33]. Through radar images, it can be observed that newly designed derivative is expected to have no oral bioavailability, less polarity, low flexibility, and low solubility.

In addition, boiled egg diagram illustrated how the ligands were absorbed in the gut and the brain. Other names for this type of graph are the Egan egg graph, the brain or intestine estimated permeation prediction model[33]. Fig. 9 displays the “boiled egg” graph of Tamoxifen along with compounds 1 and 32.

Boiled egg diagram

GI absorption and blood-brain barrier penetration

Table XII: Bioactivity score of hypothetically designed benzimidazole thiazolidinone derivatives having pyrazole as substituent (12-32)

Compound No.	G-Protein coupled receptor ligand	Ion channel modulator	Kinase Inhibitor	Nuclear receptor ligand	Protease inhibitor	Enzyme inhibitor
Tamoxifen	**0.30**	**0.00**	**-0.01**	**0.57**	**0.04**	**0.32**
12	-0.08	-0.26	-0.42	-0.51	-0.36	-0.20
13	-0.10	-0.34	-0.45	-0.53	-0.39	-0.25
14	-0.08	-0.30	-0.43	-0.52	-0.38	-0.23
15	-0.14	-0.34	-0.45	-0.58	-0.43	-0.26
16	-0.07	-0.30	-0.40	-0.49	-0.37	-0.22
17	-0.05	-0.27	-0.40	-0.42	-0.34	-0.18
18	-0.10	-0.39	-0.46	-0.52	-0.38	-0.26
19	-0.05	-0.26	-0.35	-0.55	-0.30	-0.16
20	-0.18	-0.44	-0.54	-0.60	-0.43	-0.33
21	-0.15	-0.52	-0.57	-0.54	-0.35	-0.32
22	-0.02	-0.41	-0.55	-0.72	-0.21	-0.20
23	-0.09	-0.49	-0.55	-0.49	-0.27	-0.35
24	-0.09	-0.34	-0.43	-0.50	-0.37	-0.24
25	-0.02	-0.48	-0.55	-0.71	-0.19	-0.19
26	-0.08	-0.31	-0.43	-0.51	-0.39	-0.23
27	-0.06	-0.30	-0.39	-0.47	-0.35	-0.21
28	-0.15	-0.34	-0.46	-0.58	-0.44	-0.25
29	-0.05	-0.27	-0.38	-0.41	-0.35	-0.17
30	-0.11	-0.39	-0.44	-0.52	-0.39	-0.26
31	-0.05	-0.27	-0.34	-0.54	-0.30	-0.15
32	-0.15	-0.51	-0.55	-0.53	-0.36	-0.31

are crucial steps in the drug development process. In calculating the polarity and lipophilicity of derivatives, the Boiled-egg model is helpful. In Boiled-egg diagram, the yellow section indicates a significant potential for BBB permeation, the white region represents GIT absorption, and the blue dots indicate compounds that are effectively refluxed by P-glycoprotein (PGP+), while the red dots indicate chemicals that are not P-glycoprotein substrates (PGP-). The analysis predicts that all molecules including reference tamoxifen show low GI absorption except compound 12. None of the molecules penetrate the blood-brain barrier including tamoxifen. 50% of the molecules are P-gp+, while the other 50% are P-gp-negative.

Pharmacokinetics

The free online ADME resource, SwissADME, was used to predict drug-likeness and pharmacokinetic features. The results are tabulated in Table X, XI and XII**.** These studies revealed that all compounds possessed low gastrointestinal (GI) absorption except compound 12. Tamoxifen, the reference drug, has the same profile. Almost all the compounds are not permeable to the blood-brain barrier. In spite of this, the majority of the substances inhibited the cytochrome P450 isomers (CYP2C9, CYP3A4, CYP2D6 and CYP2C19)[34]. Pains and Brenk are the two filters, these filters have comparable results to those of tamoxifen. The medicinal property screening

was also studied using Molinspiration software. All the compounds have a synthetic ability value between 4.45 and 4.71 and a bioavailability score of 0.55 similar to that of reference tamoxifen except for 20, 21, 22, and 25. The bioactivity of each compound was predicted using the online Molecular Inspiration software and are shown in Table XII. The possibility of good to mild activity for GCPR ligands, ion channel modulation, kinase antagonists, nuclear receptor ligands, and many other enzyme inhibitors was indicated by the bioactivity score of all proposed compounds. These results for organic compounds can be translated as being active (bioactivity > 0), moderately active (bioactivity score: -5.0 to 0.0), or inert (bioactivity score < -5.0)[35]. In our results, most of the compounds have a bioactivity score between -0.02 and -0.71.

Predicted physicochemical, pharmacokinetics, pharmacodynamics, characteristics of compounds (12 to 32) were found to be comparable to standard 4-hydroxy tamoxifen and make them qualified to be druggable candidates.

CONCLUSION

Breast cancer is a serious topic of concern. Globally, it has been recorded as being at the top of the list of cancers compared to other malignancies. Therefore, there is a need to develop some effective medicinal agents against breast cancer. From the literature, it was found that 2-substituted benzimidazole derivatives could potentially counteract breast cancer as an antagonist to estrogen receptor alpha. The molecular docking of 57 molecules (fifty-seven) from three different series has been directed in this work against the estrogen receptor alpha (PDB ID: 3ERT) and compared to reference 4- hydroxytamoxifen, which was used as a standard. According to the results of the analysis, the pyrazole series showed better binding affinity by interaction with estrogen receptor alpha, and the most potent compound in the pyrazole series was 32, which had a Mol dock score of -178.021. For a period of 100 ns, this substance was discovered to be extremely stable in the target receptor's active region. Even other aspects of this derivative, including H-bonding and steric interaction, are superior than the other two series in terms of their ability to block estrogen receptor alpha. Furthermore, compared to new derivatives, docking investigations of currently available breast cancer medications show poor results in terms of Mol Dock Score and H-bonding interaction. Next to this, acceptable results were received in an ADME/pharmacokinetics study of hypothetically designed benzimidazole-thiazolidinone derivatives with pyrazole in contrast to the existing drug tamoxifen. Based on the results of the current investigation, compound 32 was determined to be the most preferable pyrazole fused benzimidazole anticancer agent based on many features like binding affinity, associating residue and bio distribution. Compound 32 was also shown to have excellent pharmacokinetic properties that were almost identical to those of conventional 4-hydoxy tamoxifen. It was also found to be very stable in the target receptor's active site. As a result, the created estrogen receptor alpha inhibitors may be used for the creation of brand-new anti-cancer treatments that may cure the shortcomings of existing medication, such as drug resistance and may produces effective results. To support the therapeutic potential of these compounds against cancer*, in vivo* and *in vitro* research are still needed.

REFERENCES

1. Organization WHO. Noncommunicable Diseases (NCD). https:// wwwwhoint/gho/ncd/mortality_morbidity/en/ 2019; (Access on 19 January 2023)
2. Mathur P., Sathishkumar K., Chaturvedi M., Das P., Sudarshan K. L., Santhappan S., Nallasamy V., John A., Narasimhan S., Roselind F. S. and Icmr-Ncdir-Ncrp Investigator Group.: Cancer statistics, 2020: report from national cancer registry programme, India**, JCO Glob. Oncol**., 2020, 6,1063-1075.
3. Rani I., Kaur N., Goyal A. and Sharma M.: An appraisal on synthetic and medicinal aspects of fused pyrimidines as anti -neoplastic agents. **Anti-Cancer Agents Med Chem**. (Formerly **Curr. Med. Chem. Anticancer Agents**), 2023, 23(5),525-561.
4. Roy S. S. and Vadlamudi R. K.: Role of estrogen receptor signaling in breast cancer metastasis. **Int. J. Breast Cancer**, 2012, 2012, 654698.
5. Rani I. and Goyal A.: Role of GSK3 (glycogen synthase kinase 3) as tumor promoter and tumor suppressor–A review. **Plant Arch**., 2019, 19(2), 1360-1365.
6. Fuentes N., Nicoleau M., Cabello N., Montes D., Zomorodi N., Chroneos Z.C. and Silveyra P.: 17β-Estradiol affects lung function and inflammation following ozone exposure in a sex-specific manner. **Am. J. Physiol. Lung Cell Mol. Physiol**., 2019, 317(5), L702-L716.
7. Ballinger T.J., Meier J.B. and Jansen V.M.: Current landscape of targeted therapies for hormone-receptor positive, HER2 negative metastatic breast cancer. **Front Oncol.,** 2018, 8, 308.
8. Fontham E.T., Thun M.J., Ward E., Balch A.J., Delancey J.O. and Samet J.M.: American Cancer Society perspectives on environmental factors and cancer. **CA Cancer J. Clin.,** 2009, 59(6), 343-351.
9. Setti A., Rao V. V., Priyamvada Devi A., Pawar S.C., Naresh B. and Kalyan C.S.: Impact of aromatase protein variants and drug interactions in breast cancer: a molecular docking approach. **J. Recept. Signal Transduct. Res**., 2012, 32(4), 225-229.
10. Cancer. CCHtfB. https:// wwwwebmdcom/breast-cancer/guide/ breast-cancer-hormonetherapy-choices 2021. (Access on 19 January 2023)
11. Verma S. K., Ratre P., Jain A. K., Liang C., Gupta G.D. and Thareja S.: *De novo* designing, assessment of target affinity and binding interactions against aromatase: Discovery of novel leads

as anti-breast cancer agents. **Struct. Chem**., 2021, 32, 847-858.

12. http://www.rscb.org/pdb (Access on 19 January 2023)
13. Malik R., Mehta P., Srivastava S., Choudhary B.S. and Sharma M.: Pharmacophore modeling, 3D-QSAR, and *in silico* ADME prediction of *N*-pyridyl and pyrimidine benzamides as potent antiepileptic agents. **J. Recept. Signal Transduct. Res**., 2017, 37(3), 259-266.
14. Choudhary D., Rani I., Monga J., Goyal R., Husain A., Garg P. and Khokra S.L.: Pyrazole based furanone hybrids as novel antimalarial: A combined experimental, pharmacological and computational study. **Cent. Nerv. Syst. Agents Med. Chem.** (Formerly **Curr. Med. Chem**.Central Nervous System Agents), 2022, 22(1), 39-56.
15. Wu G, D'Agati V., Cai Y., Markowitz G., Park J.H., Reynolds D.M., Maeda Y., Le T.C., Hou H., Kucherlapati R. and Edelmann W.: Somatic inactivation of Pkd2 results in polycystic kidney disease. **Cell**, 1998,17, 93(2), 177-188.
16. Thomsen R. and Christensen M. H.: MolDock: a new technique for high-accuracy molecular docking. **J. Med. Chem.,** 2006, 49(11), 3315-3321.
17. Rani I., Kalsi A., Kaur G., Sharma P., Gupta S., Gautam R.K., Chopra H., Bibi S., Ahmad S.U., Singh I. and Dhawan M.: Modern drug discovery applications for the identification of novel candidates for COVID-19 infections. **Ann. Med. Surg**., 2022, 104125.
18 Kciuk M., Gielecińska A., Mujwar S., Mojzych M. and Kontek R.: Cyclin-dependent kinases in DNA damage response. **Biochim. Biophys. Acta. Rev. Cancer,** 2022, 1877(3),188716.
19. Rani I., Goyal A. and Sharma M.: Computational design of phosphatidylinositol 3-kinase inhibitors. **Assay Drug Dev. Techn**., 2022, 20(7), 317-337.
20. Mujwar S. and Tripathi A.: Repurposing benzbromarone as antifolate to develop novel antifungal therapy for *Candida albicans*. **J. Mol. Model**., 2022 , 28(7), 193.
21. Mujwar S.: Computational bioprospecting of andrographolide derivatives as potent cyclooxygenase-2 inhibitors. **Biomed. Biotechnol. Res. J**., 2012, 5(4),446.
22. Mujwar S., Shah K., Gupta J.K. and Gour A.: Docking based screening of curcumin derivatives: A novel approach in the inhibition of tubercular DHFR. **Int. J. Comput. Biol. Drug Des**., 2021,14(4), 297-314.
23. Sharma K.K., Singh B., Mujwar S. and Bisen P.S.: Molecular docking- based analysis to elucidate the DNA topoisomerase IIβ as the potential target for the ganoderic acid; a natural therapeutic agent in cancer therapy. **Curr. Comput. - Aided Drug Des**., 2020,16(2), 176-189.
24. Jain R. and Mujwar S.: Repurposing metocurine as main protease inhibitor to develop novel antiviral therapy for COVID-19. **Struct. Chem**., 2020, (6), 2487-2499.
25. Yang J.M. and Chen C.C.: GEMDOCK: a generic evolutionary method for molecular docking. **Proteins: Struct. Funct. Bioinformatics**, 2004, 55(2), 288-304.
26. Mujwar S. and Harwansh R.K.: *In silico* bioprospecting of taraxerol as a main protease inhibitor of SARS-CoV-2 to develop therapy against COVID-19. **Struct. Chem**. 2022, 33(5),1517-1528; PREPRINT (Version 1) available at Research Square), doi:10.21203/rs.3.rs-1308726/v1
27. Mujwar S.: Computational repurposing of tamibarotene against triple mutant variant of SARS-CoV-2. **Comput. Biol. Med**., 2021, 136,104748.
28. Thakur A., Sharma B., Parashar A., Sharma V., Kumar A. and Mehta V.: 2D-QSAR, molecular docking and MD simulation based virtual screening of the herbal molecules against Alzheimer's disorder: an approach to predict CNS activity. **J. Biomol. Struct. Dyn**., 2023, 18,1-5.
29. Mujwar S., Deshmukh R., Harwansh R.K., Gupta J.K. and Gour A.: Drug repurposing approach for developing novel therapy against mupirocin-resistant *Staphylococcus aureus*. **Assay Drug Dev. Techn**., 2019, 17(7), 298-309.
30. Accessed SIoB. http://wwwswissadmech/ 2021. (Access on 22 January 2023)
31. Piplani P., Sharma M., Mehta P. and Malik R.: *N*-(4-Hydroxyphenyl)-3, 4, 5-trimethoxybenzamide derivatives as potential memory enhancers: Synthesis, biological evaluation and molecular simulation studies. **J. Biomol. Struct. Dyn**., 2018, 36(7),1867-1877.
32. Daina A., Michielin O. and Zoete V.: SwissADME: A free web tool to evaluate pharmacokinetics, drug-likeness and medicinal chemistry friendliness of small molecules. **Sci. Rep**.,2017, 7(1), 42717.
33. Lipinski C.A., Lombardo F., Dominy B. W. and Feeney P. J.: Experimental and computational approaches to estimate solubility and permeability in drug discovery and development settings. **Adv. Drug Deliv**. **Rev**., 2012, 64, 4-17.
34. Dhevaraj J., Gopalakrishnan M. and Pazhamalai S.: Synthesis, characterization, molecular docking, ADME and biological evaluation of 3-(4-(tetrazol-1-yl) phenyl)-5-phenyl-1*H*-pyrazoles. **J. Mol. Struct**., 2019, 1193, 450-467.
35. Sadhana S., Gupta A.K. and Amita V.: Molecular properties and bioactivity score of the *Aloe vera* antioxidant compounds-in order to lead finding. **Res. J. Pharm. Biol. Chem. Sci.,** 2013, 4(2), 876-881.